

The band structure of CuInTe₂ studied by optical reflectivity

M.V. Yakushev,^{1,2,3} A.V. Mudryi,⁴ E. Kärber,⁵ P.R. Edwards⁶ and R.W. Martin⁶

¹M.N. Miheev Institute of Metal Physics of the UB RAS, 18 S. Kovalevskaya St., 620108, Ekaterinburg, Russia

²Ural Federal University, 19 Mira St., 620002 Ekaterinburg, Russia

³Institute of Solid State Chemistry of the UB RAS, 91 Pervomaiskaya St., 620990 Ekaterinburg, Russia

⁴Scientific-Practical Material Research Centre of the National Academy of Belarus, 19 P. Brovki, 220072 Minsk, Belarus

⁵Department of Materials and Environmental Technology, Tallinn University of Technology, Ehitajate tee 5, 19086 Tallinn, Estonia

⁶Department of Physics, SUPA, University of Strathclyde, G4 0NG Glasgow, UK

* michael.yakushev@strath.ac.uk

CuInTe₂ is a semiconductor with high potential for use as a thermoelectric material and as the absorber in thin film solar cells. Studying the optical reflectivity spectra of CuInTe₂ single crystals resolves resonances at 1.054 eV and 1.072 eV, which are assigned to the A and B free excitons. Photoluminescence spectra exhibited a peak due to the A free exciton at 1.046 eV. Varshni coefficients were found for both excitons. Zero temperature bandgaps $E_{gA} = 1.060$ eV and $E_{gB} = 1.078$ eV were determined for the A and B valence sub-bands, respectively. The splitting due to crystal-field Δ_{CF} and spin-orbit effects Δ_{SO} were calculated as -26.3 meV and 610 meV, respectively, using the determined E_{gA} and E_{gB} and a literature value of E_{gC} .

The ternary compound CuInTe₂ is a semiconductor with a direct bandgap E_g of 1 eV¹ and a chalcopyrite lattice structure.² It has significant potential as a thermoelectric material (TEM).³ This potential can be quantified by the value of zT ($zT = s^2 \sigma T / \kappa$, where s , σ , T , and κ are the Seebeck coefficient, electrical conductivity, absolute temperature, and thermal conductivity, respectively), which reaches 1.18 for un-doped CuInTe₂ at 850 K. This is the highest zT -value for un-doped TEMs with the diamond structure. Furthermore, theoretical studies suggest that p -type doping of CuInTe₂ can increase zT up to 1.72 (for the same temperature).⁴ Furthermore, the steepness of energy-momentum dispersion relations of CuInTe₂, experimentally determined in ref. [5], results in carrier mobility exceeding 800 cm²V⁻¹s⁻¹ which significantly greater than those observed for other chalcopyrites making this compound highly suitable for light-harvesting applications whereas the energies of its valence and conduction bands make CuInTe₂ a strong candidate as a material for converting sunlight into sustainable hydrogen energy by photoelectrocatalytic water splitting.

On the other hand, the direct bandgap, high absorption coefficient,⁶ the possibility of p -type doping by intrinsic defects make CuInTe₂ an attractive candidate for the absorber layer of solar cells. The highest conversion efficiency η , reported so far for solar cells with CuInTe₂ absorbers, is 4.13%,⁷ whereas the use of Cu(In,Ga)Te₂ absorbers increased η up to 6.19%.⁸ Further improvements in the performance of CuInTe₂-based solar cells requires a better understanding of the electronic band structure of this material similar to that achieved for other chalcopyrites such as Cu(In,Ga)Se₂.

Optical spectroscopy has been used extensively to analyse such properties.⁹ The quantity and quality of information, which can be gained from optical spectra of a semiconductor, depends very much on its structural quality. At low defect concentrations optical spectra exhibit sharp excitonic features providing a wealth of accurate data on the electronic structure and defect nature. The presence of excitons in optical spectra and the width of their features can be used as indicators of the structural quality.¹⁰

In the early studies of the chalcopyrites CuInSe₂, CuGaSe₂ and CuInS₂ free excitonic features in reflectivity spectra were used to analyse their electronic band structure.^{2,11-13} Results of these studies made possible the successful application of Cu(In,Ga)(SeS)₂ (CIGS) in the absorber layer of thin film solar cells demonstrating conversion efficiencies η up to 22.6%,¹⁴ which is a current record for laboratory size single junction thin film photovoltaic devices.¹⁵

As with other chalcopyrites the band structure of CuInTe₂ is strongly influenced by the hybridisation of the Cu d - and the chalcogen (Te) p -states.¹⁶ The difference in the Cu-Te and In-Te

bonding generates a tetragonal distortion τ , defined as $\tau = 1 - c/2a$, where c and a are the lattice constants, which splits the uppermost valence band in the A, B and C sub-bands.

Room temperature electro-reflectance (ER) spectra of CuInTe₂ single crystals revealed an intense excitonic feature at 1 eV, which was assigned to unresolved AB free excitons and related to an E_g of 1.064 eV.¹ The C free exciton was also observed in the ER spectra at 1.674 eV. A value of $E_g = 1.061$ eV was determined in ref. [17] using optical absorption of CuInTe₂ thin films at room temperature. Optical absorption measurements at 10 K resulted in a spread of E_g values from 1.007 eV to 1.059 eV¹⁸ demonstrating how the optical bandgap, measured using absorption techniques, can be influenced by band tails generated by deep potential fluctuations at high concentrations of defects. A free exciton, observed at 1.053 eV in photoluminescence (PL) spectra, measured at 10 K in excitonic quality single crystals of CuInTe₂ has been assigned to the ground state of the A free exciton leading to an estimate of 1.059 eV for the bandgap of the A sub-band assuming a binding energy of 6 meV.¹⁹ Room temperature measurements demonstrate a reduction of E_g .⁵ However, no reports on CuInTe₂, exhibiting clear splitting of the A and B free excitons, can be found in the literature as yet.

In this paper we examine the electronic structure in excitonic grade CuInTe₂ single crystals using optical reflectivity (OR) and PL.

Single crystals of CuInTe₂ were grown from a near stoichiometric charge of the high purity elements Cu, In, and Te by the vertical Bridgman technique. A procedure, originally developed to grow high quality single crystals of CuInSe₂,²⁰ was used to grow CuInTe₂, assuming a melting point of 798 °C and the phase transition at 672 °C from the phase diagram in ref. [21].

Wavelength dispersive X-ray (WDX) microanalysis was carried out to examine the elemental composition of the samples using an electron beam energy of 10 keV and pure Cu, In and Te as standards.

A single grating monochromator with 1 m focal length was used to carry out the PL and OR measurements. The 514 nm line of an Ar⁺ laser was employed to excite PL, whereas a 100 W tungsten halogen lamp was used for the OR measurements. A closed-cycle helium cryostat was employed to hold the samples at temperatures from 5 K to 300 K. A cooled InGaAs photomultiplier tube was used to detect the PL and OR signals in the spectral region from 0.9 μ m to 1.7 μ m. The measurements were carried out with a spectral resolution of 0.4 meV. More experimental details on the optical spectroscopy set up can be found elsewhere.^{22,23}

X-ray diffraction (XRD) patterns were recorded by a Rigaku Ultima IV powder diffractometer in the Bragg-Brentano (θ - 2θ) geometry using a Cu $K\alpha_1$ radiation source ($\lambda = 0.15406$ nm). The

crystal structure and phase composition were analysed using Rigaku PDXL 2 software.

The WDX measured elemental composition of the samples (Cu: 25.4, In: 25.3 and Te: 49.3 At.%) demonstrated a near stoichiometric content of copper [Cu]/[In] = 1.00 and a slight deficiency of tellurium with respect to the metals [Te]/[Cu+In] = 0.97.

A XRD powder diffractogram, measured for the studied CuInTe₂ samples, is shown in FIG.1. This diffractogram exhibits only chalcopyrite structure reflexes of CuInTe₂ demonstrating the single-phase nature of the fabricated material. A Rietveld refinement, performed for the observed reflexes, confirmed that this material crystallised in the *I*-42d chalcopyrite phase with unit cell parameters $a = 0.6194$ nm and $c = 1.2416$ nm which result in a small and negative tetragonal distortion of - 0.23%.

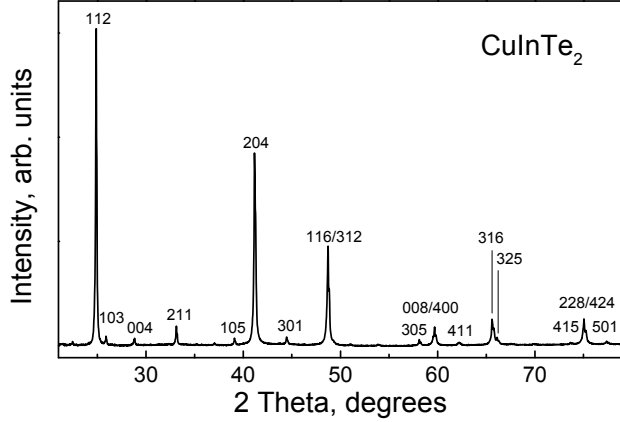


FIG.1. XRD pattern of CuInTe₂.

FIG.2 shows the near band edge region of unpolarised OR and PL spectra measured at 5 K. The PL spectrum shows a number of sharp peaks. The highest energy peak (FX) at 1.053 eV is assigned to a free exciton (FX) and has a full width at half maximum (FWHM) of 3 meV whereas the other six peaks (1 at 1.046 eV, 2 at 1.045 eV, 3 at 1.042 eV, 4 at 1.037 eV, 5 at 1.033 eV and 6 at 1.031 eV) are sharper and are likely to be attributed to bound exciton transitions.

The OR spectrum reveals two clear resonances: the A resonance with its minimum at 1.055 eV and the B resonance at 1.073 eV. The spectral position of the A resonance corresponds to that of FX in the PL spectra suggesting that FX can be assigned to the A free exciton comprising an electron from the conduction band and a hole from the A valence sub-band.

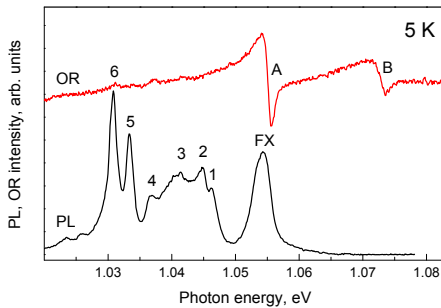


FIG.2. OR and PL spectra measured at 5 K.

The spectral energy of this peak is equal to that of the A free exciton, reported in ref. [19], supporting this assignment. The presence of excitons with a FWHM of 3 meV for the FX peak in the PL spectra demonstrates the high structural quality of this material.

We assign the B resonance to the B free exciton, a recombination of free electron from the conduction band and a hole from the B valence sub-band. FIG.3 shows an evolution of the OR spectra of the A and B excitons at temperature increasing from 5 K to 180 K.

It can be seen that both the A and B resonances gradually redshift with rising temperature. Both resonances broaden with rising temperatures and are not resolved for beyond 160 K.

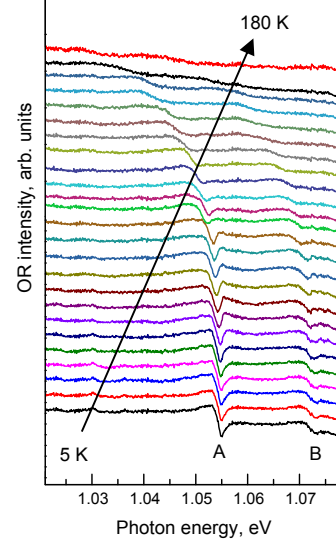


FIG.3. Temperature dependence of the A and B free exciton region of the OR spectra.

To accurately determine the spectral position of the excitons the OR spectra were fitted with the function proposed in ref. [24]:

$$R(E) = R_0 + R_x \left(R e^{i\theta} \frac{(E_x - E + i\Gamma_x)}{[\Gamma_x^2 + (E_x - E)^2]} \right), \quad (1)$$

where E_x is the A or B excitons spectral energy, Γ_x is the broadening parameter of the exciton and θ is a phase, whereas R_x is an amplitude and R_0 a background.

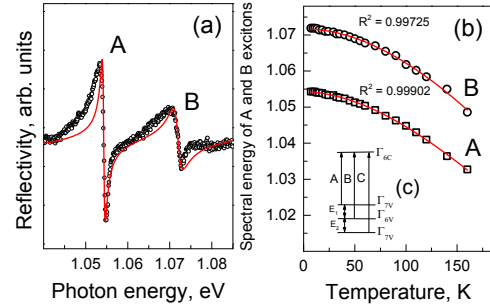


FIG.4. (a) OR spectrum measured at 5 K (○) and fitted with eq. (1) (-red line). (b) temperature dependence of the spectral position of the A(□) and B(○) excitons in the OR spectra and the best fits using the Varshni expression (red lines), (c) the energy band structure of CuInTe₂ at the centre of the Brillouin zone (not drawn to scale).

An example of the fitting for the 5 K OR spectrum is shown in FIG.4(a). FIG.4(b) shows the temperature dependence of the spectral energy of the A and B excitons in the OR spectra. The experimental points were fitted with the Varshni expression:²⁵

$$E_{FX}(T) = E_{FX}(0) - \alpha T^2 / (\beta - T), \quad (2)$$

where $E_{FX}(T)$ is the spectral energy of the A or B exciton at temperature T , $E_{FX}(0)$ is this energy at 0 K, α and β are fitting parameters. The fitting parameters for both excitons are collected in Table I.

Neither of the E_{gA} and E_{gB} temperature dependencies shown in FIG.4(b) demonstrates the non-monotonic change of the bandgap observed at low temperatures for CuInSe₂²⁶ and CuInS₂²⁷. The character of the temperature dependence of E_g is attributed to the combined effect of temperature changes of the lattice constants and electron-phonon interaction.

Assuming a binding energy of 6 meV for both the A and B excitons, as estimated in ref. [18], we can determine 0 K values of the A and B bandgaps as $E_{gA} = 1.060$ eV and $E_{gB} = 1.078$ eV.

Table I. Varshni α and β fitting parameters as well as zero temperature spectral energy $E_{FX}(0)$ for the A and B free excitons.

Exciton	α , eV/K	β , K	$E_{FX}(0)$, eV
A	$(4.1 \pm 0.4)10^{-4}$	327 ± 45	1.0542 ± 0.0004
B	$(7.0 \pm 0.2)10^{-4}$	640 ± 227	1.0717 ± 0.0001

A quasi-cubic model, developed by Hopfield²⁸ for binary hexagonal semiconductors, interprets the valence band splitting as a result of the simultaneous influence of the spin-orbital Δ_{SO} and crystal field coupling Δ_{CF} . Although the model failed to produce accurate theoretical values of Δ_{SO} and Δ_{CF} for the Cu-III-VI₂ chalcopyrites^{2,29} due to a hybridisation of the Cu *d*- and *p*-states of other atoms such an interpretation has been used in a number of papers concerned with the electron structure of semiconductor compounds. Experimentally Δ_{SO} and Δ_{CF} can be determined from E_{gA} , E_{gB} and E_{gC} , the A, B and C sub-bandgaps of CuInTe₂, as follows:²⁸

$$\Delta_{SO} = -\frac{1}{2}(E_1 + E_2) + \frac{1}{2}[(E_1 + E_2)^2 - 6E_1E_2]^{1/2}, \quad (3)$$

and

$$\Delta_{CF} = -\frac{1}{2}(E_1 + E_2) - \frac{1}{2}[(E_1 + E_2)^2 - 6E_1E_2]^{1/2}, \quad (4)$$

where $E_1 = E_{gB} - E_{gA}$ and $E_2 = E_{gB} - E_{gC}$. Using the E_{gA} and E_{gB} values, determined in this study, and an E_{gC} of 1.674 eV from ref. [1], $\Delta_{CF} = -26.3 \pm 0.4$ meV and $\Delta_{SO} = 610 \pm 20$ meV, were calculated. A schematic energy band structure of CuInTe₂ at the centre of the Brillouin zone is shown in FIG.4(c).

The previously reported values of the crystal-field and spin-orbit splitting in CuInTe₂ $\Delta_{CF} = 0$ meV and $\Delta_{SO} = 610$ meV, respectively, were estimated in ref. [17] assuming zero splitting of the A and B valence sub-bands. Such a splitting directly determines Δ_{CF} , whereas the value of Δ_{SO} , calculated in this paper, is in excellent agreement with our value demonstrating its weak sensitivity to the non-cubic deformation of the lattice along with the A-B sub-band splitting, generated by this deformation. **Angle-resolved photoelectron spectroscopy measurements⁵ also show a similar band structure: a clear C valence sub-band splitting and probably a sign of the A-B sub-band separation. Since $\Delta_{CF} \ll \Delta_{SO}$, the literature value of 610 meV¹ we used can be compared to the estimate of Δ_{SO} of approximately 800 meV in Ref. 5, although the temperature and formalism are different.**

The tetragonal distortion reported for CuInSe₂ in ref. [30] is -0.48%, which is close to that of τ , measured for CuInTe₂ in this paper. However, in CuInTe₂ its small and negative τ results in the small and negative Δ_{CF} whereas in CuInSe₂ $\Delta_{CF} = 5.3$ meV is positive due to the inversion of its upper most valence sub-bands.²⁶ The spin orbital splitting in CuInSe₂ of 234.7 meV, also reported in ref. [26], is significantly smaller than that in CuInTe₂.

The tetragonal distortion of 1.87% in another technologically important chalcopyrite CuGaSe₂, reported in ref. [31], is positive and its magnitude is significantly greater than that in CuInTe₂. Such a positive τ results in CuGaSe₂ in a negative $\Delta_{CF} = -112$ meV,¹² which is much greater than that determined in this paper for CuInTe₂. A spin-orbit splitting of 231 meV, reported for CuGaSe₂ in the same report, is significantly smaller than our finding for CuInTe₂. The character of the energy band structure of CuInTe₂ at the centre of the Brillouin zone is similar to that of CuGaSe₂.¹²

Although the **measured** splitting of the A and B valence sub-bands does not provide an immediate solution to technological problems of the fabrication of CuInTe₂-based solar cells or thermoelectric devices this result should improve the general level of understanding of the electronic properties of the compound

accelerating the development process of efficient CuInTe₂-based electronic devices.

In conclusion, the electronic band structure of CuInTe₂ single crystals, grown by the vertical Bridgman technique, was studied by OR and PL. The 5 K PL spectra showed sharp peaks assigned to excitonic recombination. The 5 K OR spectra revealed two resonances, A at 1.054 eV and B at 1.072 eV, assigned to the A and B free excitons. Varshni coefficients were found for both excitons. Bandgaps of $E_{gA} = 1.060$ eV and $E_{gB} = 1.078$ eV, for the A and B valence sub-bands, respectively, were determined for zero temperature assuming a binding energy of 6 meV. The splitting due to crystal-field Δ_{CF} and spin-orbital effects Δ_{SO} were calculated as -26.3 meV and 610 meV, respectively, using the determined E_{gA} , E_{gB} and a literature value of E_{gC} .

The optical spectroscopy studies were supported by the Russian Science Foundation (grant 17-12-01500), XRD measurements were supported by the Estonian Ministry of Education and Research project IUT19-4.

¹M.J. Thwaites, R.D. Tomlinson, M.J. Hampshire, *Solid State Commun.* **23**, 905 (1977).

²J.L. Shay, J.H. Wernick, *Ternary Chalcopyrite Semiconductors. Growth, Electronic Properties and Applications* (Pergamon, 1975).

³R. Liu, L. Xi, H. Liu, X. Shi, W. Zhang and L. Chen, *Chem. Commun.* **48**, 3818 (2012).

⁴G.Zhou, D.Wang, *Phys. Chem. Chem. Phys.* **18**, 5925 (2016).

⁵J.J. Frick, A. Topp, S. Klemen, M.S. Krivenkov, A.Y. Varykhalov, C. Ast, A.B. Bocarsly, L.M. Schoop, *The Journal of Physical Chemistry Letters* **9**, 6833 (2018).

⁶D. Sridevi, K. V. Reddy, *Thin Solid Films* **141**, 157 (1986).

⁷M. Lakhe, N.B. Chaurse, *Solar Energy Materials and Solar Cells* **123**, 122 (2014).

⁸M.M.S. Sanad, M.M. Rashad, A.Y. Shenouda, *International Journal of Electrochemical Science*, **11**, 4337 (2016).

⁹H.B. Bebb, E. Williams, *Semiconductors and Semimetals* (Academic Press).

¹⁰E.H. Bogardus and H.B. Bebb, *Phys. Rev. B*, **176**, 994 (1968).

¹¹J.L. Shay, B. Tell, H.M. Kasper and L.M. Schiavon, *Phys. Rev. B* **7**, 4485 (1973).

¹²B. Tell and P.M. Bridenbaugh, *Phys. Rev. B* **12**, 3330 (1975).

¹³B. Tell, J.L. Shay, H.M. Kasper, R.L. Barns, *Phys. Rev. B* **10**, 1748 (1974).

¹⁴P. Jackson, R. Wuerz, D. Hariskos, E. Lotter, W. Witte, M. Powalla, *Phys. Status Solidi RRL* **10**, 583 (2016).

¹⁵M.A. Green, Y. Hishikawa, E.D. Dunlop, D.H. Levi, J. Hohl-Ebinger, A.W.Y. Ho-Baillie, *Prog. Photovolt. Res. Appl.*, **26**, 3 (2018).

¹⁶J. E. Jaffe and A. Zunger, *Phys. Rev. B* **29**, 1882 (1984).

¹⁷H. Neumann, B. Perlst and W. Horig, *Thin Solid Films* **182**, 115 (1989).

¹⁸G. Marin, C. Rincon, S. M. Wasim, Ch. Power, and G. S. Perez, *J. Appl. Phys.* **81**, 7580 (1997).

¹⁹C. Rincón, S. M. Wasim, G. Marin, G. Sánchez Pérez, and G. Bacquet, *J. Appl. Phys.* **82**, 4500 (1997).

²⁰R.D. Tomlinson, *Solar Cells* **16**, 17 (1986).

²¹L.S. Palatnik and E.I. Rogachova, *Soviet Physics - Doklady* **12**, 503 (1967).

²²M.V. Yakushev, A.V. Mudryi, O.M. Borodavchenko, V.A. Volkov and R.W. Martin, *J. Appl. Phys.* **118**, 155703 (2015).

²³M.V. Yakushev, J. Krustok, M. Grossberg, V.A. Volkov, A.V. Mudryi, and R.W. Martin, *J. Phys. D: Appl. Phys.* **49**, 105108 (2016).

²⁴K.P. Korona, A.W. Aysmolek, K. Pakula, R. Stepniewski, J. M. Baranowski, I. Grzegory, B. Lucznik, M. Wroblewski, and S. Porowski, *Appl. Phys. Lett.* **69**, 788 (1996).

²⁵Y.P. Varshni, *Physica* **34**, 149 (1967).

²⁶A.V. Mudryi, M.V. Yakushev, R.D. Tomlinson, I.V. Bodnar, I.A. Viktorov, V.F. Gremenok, A.E. Hill, R.D. Pilkington, *Appl. Phys. Lett.* **77**, 2542 (2000).

²⁷M.V. Yakushev, A.V. Mudryi, I.V. Victorov, J. Krustok, E. Mellikov, *Appl. Phys. Lett.* **88**, 011922 (2006).

²⁸J.J. Hopfield, *J. Phys. Chem. Solids* **15**, 97 (1960).

²⁹N. Yamamoto, H. Horinaka, K. Okada, and T. Miyauchi, *Japan. J. Appl. Phys.* **16**, 1817 (1977).

³⁰J. Parkes, R.D. Tomlinson, M.J. Hampshire, *J. Appl. Crystallogr.* **6**, 414 (1973).

³¹L. Mandel, R.D. Tomlinson, M.J. Hampshire, *J. Appl. Crystallogr.* **10**, 130 (1977).

